Gene 699 (2019) 16–23

Contents lists available at ScienceDirect

Gene

journal homepage: www.elsevier.com/locate/gene

Research paper

Identification of a homozygous GFPT2 variant in a family with asthenozoospermia

Masomeh Askari[a], Dor Mohammad Kordi-Tamandani[a,*], Navid Almadani[b], Kenneth McElreavey[c], Mehdi Totonchi[b,**]

[a] Department of Biology, University of Sistan and Baluchestan, Zahedan, Iran
[b] Department of Genetics at Reproductive Biomedicine Research Center, Royan Institute for Reproductive Biomedicine, ACECR, Tehran, Iran
[c] Human Developmental Genetics, Institute Pasteur, Paris, France

ARTICLE INFO

Keywords:
Asthenozoospermia
Whole-exome sequencing
GFPT2
Reactive oxygen species

ABSTRACT

Purpose: Asthenozoospermia (ASZ) is a condition characterized by reduced sperm motility in semen affecting approximately 19% of infertile men. Major risk factors, particularly gene mutations, still remain unknown. The main aim of the present study was to identify novel genes and mutations that may influence human sperm motility.

Methods: Whole-exome sequencing (WES) was performed on a large pedigree of infertile men (n = 5) followed by bioinformatics analyses. Candidate pathogenic variants were screened in a control cohort of 400 ancestry-matched Iranian fertile men, 30 unrelated men with idiopathic ASZ, and public databases.

Results: A rare mutation in GFPT2 gene (c.1097G > A; p.Arg366Gln) located in the SIS 1 domain was segregated with the phenotype and was consistent with autosomal recessive inheritance. The *in silico* analyses revealed that the mutation might affect the function of SIS 1 domain and abolish its carbohydrate-binding ability.

Conclusion: Homozygosity of the GFPT2 p.Arg366Gln mutation was associated with increased levels of reactive oxygen species (ROS) in spermatozoa and decreased sperm motility.

1. Introduction

Infertility is a condition identified as inability to get pregnant after at least one year of regular unprotected sexual intercourse (Pfeifer et al., 2015). This reproductive disorder affects 15% of couples, with male infertility attributing to approximately 50% of all recorded cases (Agarwal et al., 2015). The causes of male infertility are semen anomalies, impaired spermatogenesis or spermiogenesis, and genital tract obstruction (Matzuk and Lamb, 2008). Various factors are involved in male fertility, sperm motility being considered one of the most important ones (kumar Mahat and Arora, 2016). Studies have indicated that sperm motility is associated with three main factors including: flagellar ultrastructure, phosphorylation and glycolysis mediated by ATP, and metabolic pathways such as cAMP-dependent protein kinase and calcium signaling pathway (Pereiraa et al., 2014). Genetic variations in genes related to these biological pathways can profoundly influence male fertility. Accordingly, The World Health Organization (WHO) has categorized spermatozoa as progressive motile (PR), non-progressive motile (NP), and immotile (IM). Poor sperm motility is diagnosed when total motility (PR + NP) is < 40% or progressive motility (PR) is < 32%. Asthenozoospermia (ASZ), which is characterized by reduced sperm motility, is considered as an isolated disorder, combined with other sperm anomalies or syndromic associations (Luconi et al., 2006). Isolated ASZ accounts for 19% of male infertility; however, ASZ is also detected in nearly 64% of infertile men with oligozoospermia “low level of sperm” or teratozoospermia “sperm morphological abnormalities” (Curi et al., 2003).

ASZ is of multifactorial etiology and may result from prolonged sexual abstinence, sperm dysfunction, varicocele, genital tract infections, and genetic factors, as well as unhealthy lifestyle (Zuccarello

Abbreviations: ASZ, Asthenozoospermia; NGS, Next Generation Sequencing; WES, Whole-Exome Sequencing; ROS, Reactive Oxygen Species; ART, Assisted Reproduction Technology; YCDM, Y Chromosome Microdeletions; GFPT2, Glutamine-Fructose-6-Phosphate Transaminase 2; SIS 1, Sugar Isomeras 1; PBS, Phosphate-Buffered Saline

* Correspondence to: D.M. Kordi-Tamandani, Department of Biology, University of Sistan and Baluchestan, P.O. Box: 16835-128, Zahedan, Iran.
** Correspondence to: M. Totonchi, Genetics and Stem Cell Departments, Royan Institute, P.O.Box: 16635-148, Tehran, Iran.
E-mail addresses: dor_kordi@science.usb.ac.ir (D.M. Kordi-Tamandani), m.totonchi@royaninstitute.org (M. Totonchi).
URL: http://www.RoyanInstitute.org (M. Totonchi).

https://doi.org/10.1016/j.gene.2019.02.060
Received 22 July 2018; Received in revised form 12 February 2019; Accepted 22 February 2019
Available online 05 March 2019
0378-1119/

et al., 2008). The underlying causes of ASZ have not been identified in most cases although genetic factors are thought to be important (Bracke et al., 2018). In mice more than fourteen genes are associated with altered sperm motility (Matzuk and Lamb, 2008); only few of these genes, however, have been shown to be associated with human ASZ (Bracke et al., 2018). Genetic studies have identified mutations in sperm-specific ion exchanger, channels and structural proteins (*i.e. SLC26A8* (MIM #608480) encoding anion transporter, *CATESPER1-2* (MIM #606389 and MIM #607249) encoding cation channel and *SEPT12* (MIM #611562) encoding protein subunits of the annulus (Avenarius et al., 2009; Dirami et al., 2013; Kuo et al., 2012).

Assisted reproduction technology (ART) can be used for patients affected with ASZ. However, the ART outcomes while utilizing low-motility spermatozoa compared to normal-motility spermatozoa show significant reductions in the rates of fertilization and pregnancy and in embryo qualities (Bhilawadikar et al., 2013). Understanding the genetic etiology of ASZ not only increases ART success but also prevents the transmission of causal mutations to offspring. Genetic studies of male infertility can prove difficult in some cultures since it may be considered a social stigma. Because of the heterogeneous nature of infertility (Krausz et al., 2015), candidate gene approaches have not been particularly successful (Gilissen et al., 2012). Family-based whole-exome sequencing (WES) has led to the identification of the causal mutation in a number of families with male infertilities involving the genes *DNAH1* (MIM #603332) and *SPAG17* (MIM #616554) (Amiri-Yekta et al., 2016; Xu et al., 2017).

In the present study, family-based WES was applied to uncover underlying mutations in two consanguineous families suffering from ASZ with zero progressive motile spermatozoa and high concentrations of spermatozoal reactive oxygen species (ROS). A homozygous missense variant in *GFPT2* was identified as the pathogenic candidate. *In silico* analyses demonstrated that this variant in *GFPT2* affected SIS 1 function.

2. Material and methods

2.1. Subjects

Two consanguineous Iranian families with five infertile men underwent investigation at the Infertility Clinic & Reproductive Biomedicine Research Center of Royan Institute, Tehran, Iran (Fig. 1). All infertile men were subject to complete andrological examinations with respect to their medical history, current well-being as well as hormonal and semen analyses. Serum concentrations of follicle stimulating hormone (FSH), luteinizing hormone (LH) and testosterone were evaluated using Elecsys and Cobas e411 analyzers (Roche, Germany). After 2–7 days of sexual abstinence, semen samples were collected and analyzed in compliance with WHO guidelines. After liquefaction of samples within 30 min at 37 °C, seminal plasma quality in

Table 1
Personal medical history and physical examination of five patients in the pedigree with asthenozoospermia.

Medical history	III-2	III-6	III-9	III-13	III-16
Infectious medical history	–	–	–	–	–
Cryptorchidism	–	–	–	–	–
Surgical scar	–	–	–	–	–
Toxic/heat exposure	–	–	–	–	–
Vasectomy	–	–	–	–	–
Physical examination					
General appearance	N	N	N	N	N
Testis volume & position	N	N	N	N	N
Epididymis volume & position	N	N	N	N	N
Hydrocele, varicocele, cyst	N	N	N	N	N
Vas deferens	N	N	N	N	N
Scortum	N	N	N	N	N
N(Normal)					

Table 2
Semen and hormone analysis of five p[patients in the pedigree with asthenozoospermia.

Semen parameters	III-2	III-6	III-9	III-13	III-16
Volume (N: 2–7 CC)	2	6	4	5	6
PH (N:7.2–8)	7.8	7.7	7.8	7.7	7.8
Sperm count (N: $> 20 \times 10^6$/m)l	72	32	45	56	38
Sperm motility, Total (N: 40–100%)	12	13.5	14.9	11	10
Rapid progressive; Class A	0	0	0	0	0
Non-motile: Class D (N: 0–60%)	88	86.5	85.1	81	90
Normal morphology (N:4–100)	5	7	10	5	4
Hormone analysis					
LH (N:7.2–7 CC)	4.5	5.98	4.7	4.8	5.08
FSH(N: 2–10 mIu/ml)	2.6	3.81	4.6	3.5	2.58
Testosterone (N: > 2.4 ng/ml)	5.1	5.4	4.1	4.3	5.35

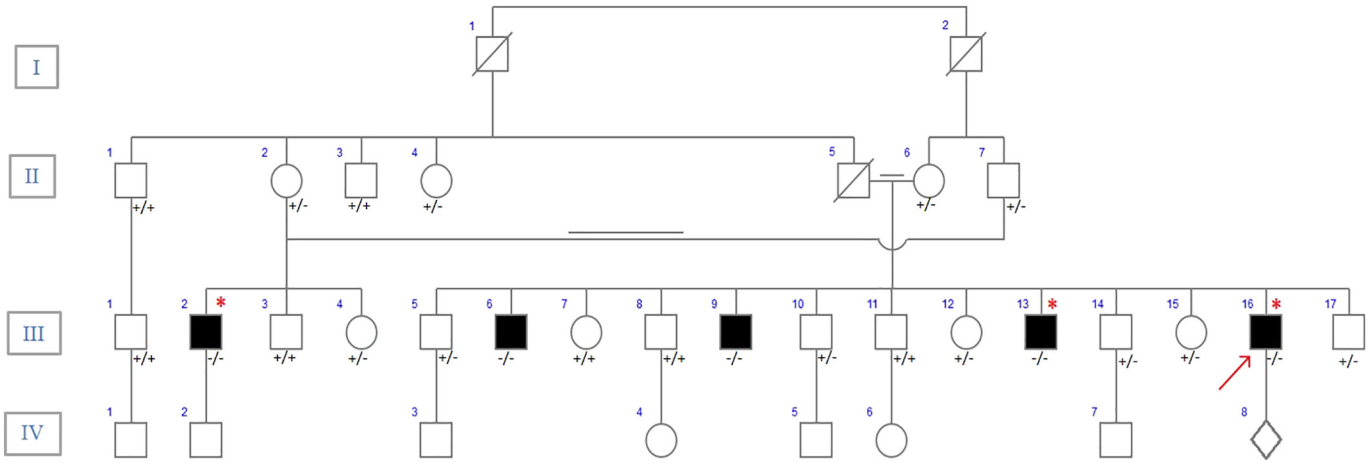

Fig. 1. Pedigree of multiplex consanguineous family with asthenozoospermia. Black and white squares represent infertile and fertile men respectively. The proband is indicated by a red arrow. Affected men who underwent whole exome sequencing are indicated by a red asterisk. +/+ indicates reference genotype, +/− indicates heterozygosity for the mutation and −/− indicates homozygous mutation genotype. (For interpretation of the references to colour in this figure legend, the reader is referred to the web version of this article.)

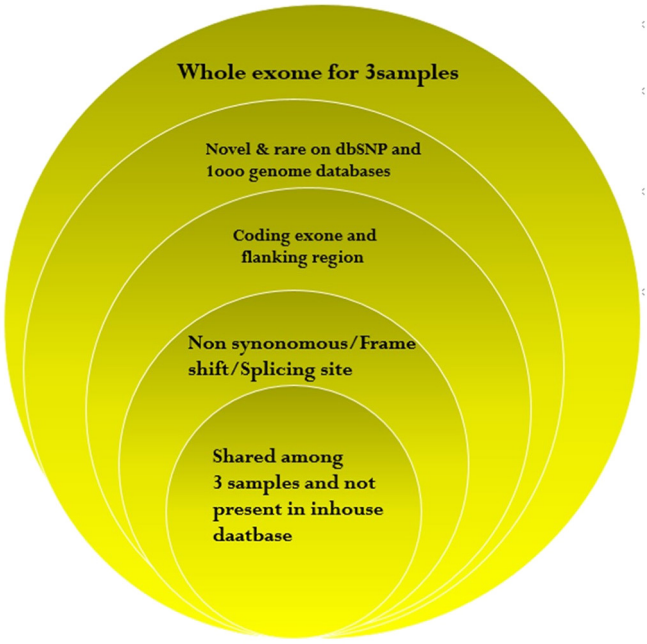

Fig. 2. Schematic representation of the variant filtering process of WES-based identified variants. In the first step, common variants (minor allele frequency (MAF) > 0.01) were filtered. In the second step, intronic, 5'UTR and 3'UTR were excluded. After excluding non-pathogenic variants, novel/rare and shared variants were selected.

terms of volume, pH, viscosity, and leukocytes count were determined. Furthermore, the spermatozoa concentration, motility and morphology were also analyzed by a computer-assisted semen analyzer (CASA) system.

Genetic screening was done for all patients using karyotyping and Y chromosome microdeletions (YCMD) test. Karyotype analysis was carried out on lymphocytes collected from the peripheral blood, using standard G-banding technique and the YCMD test was conducted by multiplex PCR assay. A 5 ml blood sample was taken from each man and 31 available family members for genomic DNA extraction. All individuals who agreed to participate in this study submitted the informed consent. This study was approved by the Institutional Review Board of the Royan Institute Research center and Royan Ethics Committee, Tehran, Iran.

2.2. Whole-exome sequencing and bioinformatics analyses

Genomic DNA (gDNA) was extracted from peripheral blood lymphocytes using the standard salting-out method. Three samples of gDNA (III-2, III-13 and III-16) were subject to WES. Then, the following steps were taken. First, 1 µg DNA was sheared to 120–200 bp fragments by sonication and exome capture was carried out using the Agilent SureSelect Human All Exon 1.2 kit. Additionally, paired-end sequencing was applied on the illumina HiSeq 2000 platform by TruSeq v3 chemistry. Read files (Fastq) were generated from the sequencing platform *via* the manufacturer's proprietary software. Reads were aligned to human reference genome (hg19) with the Burrows-Wheeler Aligner (BWA) package version 0.7.10 (Li and Durbin, 2009). The duplicate read pairs, were marked using Picard version 1.107. The additional BAM file manipulations were conducted by Samtools 0.1.18. Base quality recalibration was performed using GATK's covariance

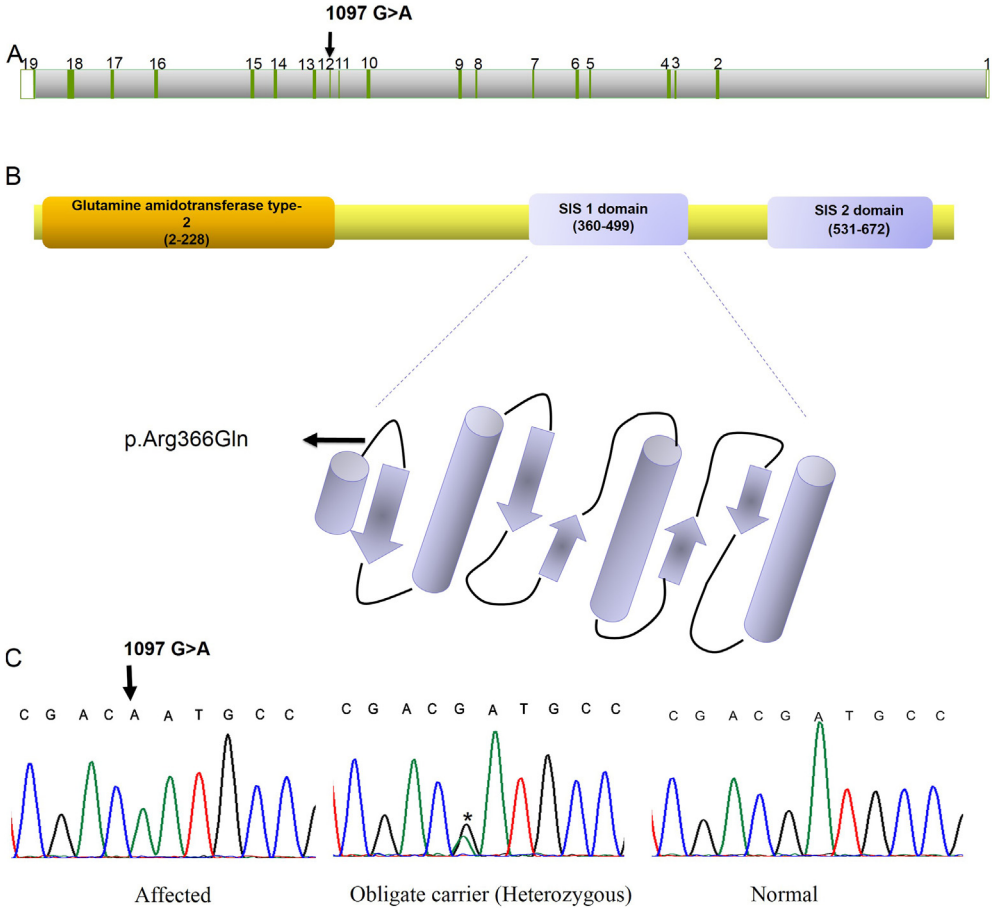

Fig. 3. Location and conservation of GFPT2 mutation. (A) Schematic of the human GFPT2 gene; the position of coding exon is demonstrated by green boxes. (B) CLDN2 protein structure, p.Arg366Gln located in coil structure in SIS 1 domain. (C) Sequence electropherogram of coding exon of CLDN2 amplified from genomic DNA of affected, normal and obligate carrier family members. Site of mutation marked by black arrow and heterozygous missense mutation is indicated by black asterisk. (For interpretation of the references to colour in this figure legend, the reader is referred to the web version of this article.)

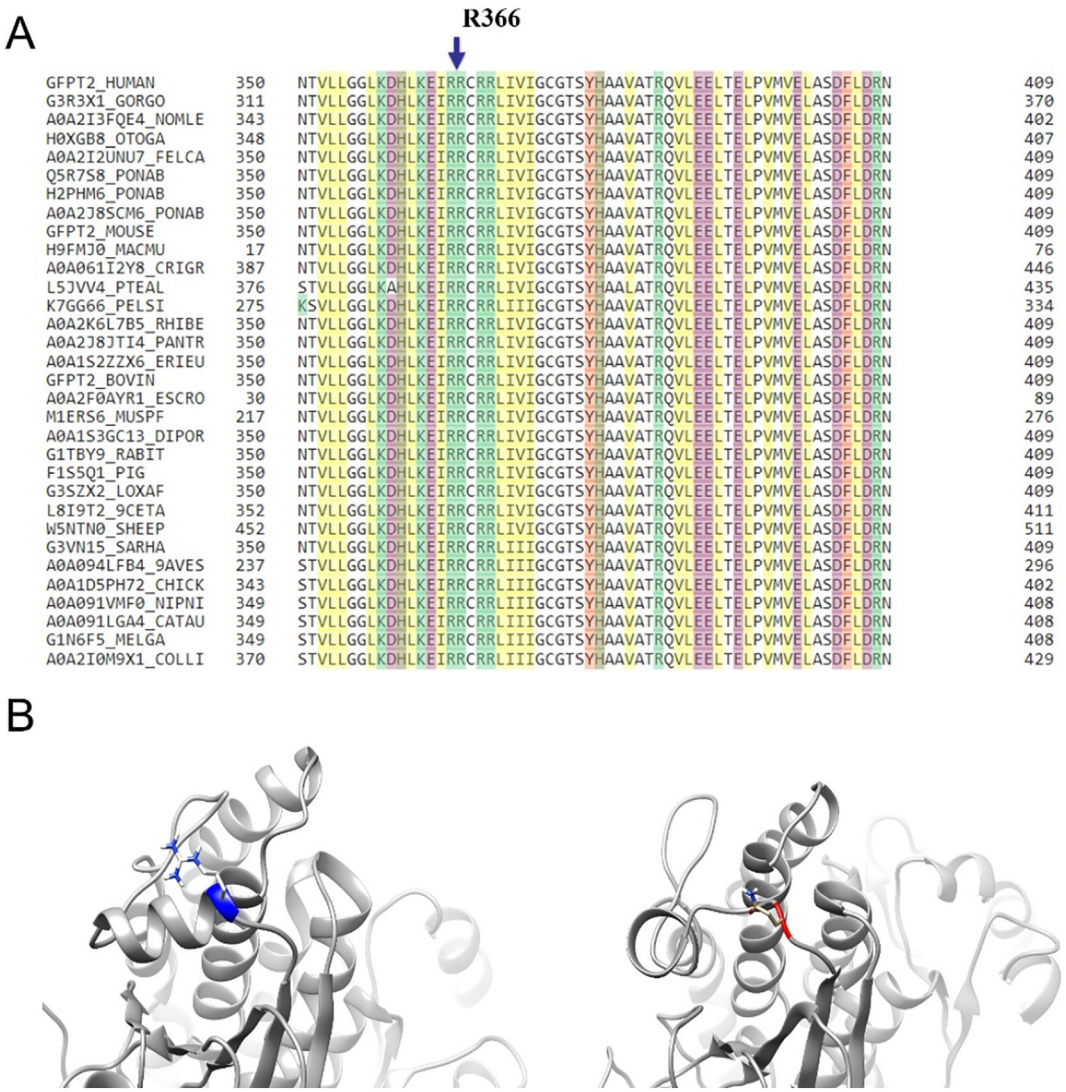

Fig. 4. Conservation and *in silico* analysis of GFPT2 mutation. (A) Multiple sequence alignment shows conservation amino acid (p.R366) across species (conserved amino acid is shown by black arrow). (B) Molecular view of the p.Arg366Gln. The protein is colored dark blue and purple, the side chains of both the wild-type and the mutant residue are shown colored green and red respectively. (For interpretation of the references to colour in this figure legend, the reader is referred to the web version of this article.)

recalibration (McKenna et al., 2010). SNP and indel variants were called and annotated by haplotype caller (DePristo et al., 2011) and ANNOVAR for each sample (Wang et al., 2010). Both dbSNP release 138 and ExAC database were used to obtain novel and rare variants with frequency < 0.005. Also, novel/rare variants were filtered out against an in-house database containing variants from 400 exomes of fertile men. In both coding and splice site regions, variants were prioritized based on being nonsynonymous, indel and putative splice site. Notably, variants shared by the three cases were retained for further analysis. In order to determine the severity of the effect of candidate variants, *in silico* analysis was done using Sift, PolyPhen2, mutation taster and HOPE (Venselaar et al., 2010).

2.3. Sanger sequencing validation and segregation analyses

Validation and segregation of *GFPT2* (NM_005110.3) variant, located on exon 12, were made by PCR-amplified gDNA from three patients (namely, III-2, III-13 and III-16) and their family members (Fig. 1) as well as 30 idiopathic ASZ ones. Thermo cycler standard conditions were optimized for amplification of forward (5'-TTCAATACTATGAGA GGTCGGG-3′) and reverse (5-CAGTGTCTGGTCCTAGACTG-3′) primers which had been designed by PerlPrimer software. The 296-bp amplicons were Sanger sequenced with Macrogen (Seoul, Korea). The data were aligned with human reference genome (hg19/b37) and analyzed by Sequence Scanner (Version 1.0).

2.4. In silico prediction 3D structure of native and mutant type of GFPT2 protein

A homology model of wild and mutant GFPT2 was developed by the program Phyre2 (Kelley et al., 2015) and the effects of altered residues on the protein structures was visualized by program PyMol viewer (DeLano, 2002). Molecular dynamic (MD) simulations were carried out using the GROMACS 5.1.4 package and GROMACS 54A7 force field (Van Der Spoel et al., 2005). All the systems were primarily solvated in SPC/E water mode and neutralized with counter ions in cubic boxes with length of 7.7 nm (Hoover, 1985; Parrinello and Rahman, 1981). The temperature was set at 310 K using the Nose–Hoover algorithm with a 0.1 ps coupling constant (Mark and Nilsson, 2001; Nosé and Klein, 1983). The pressure was maintained at 1 bar with a isotropic Parrinello–Rahman algorithm with a 0.5 ps coupling (Parrinello and Rahman, 1981). All MD simulations were performed under periodic

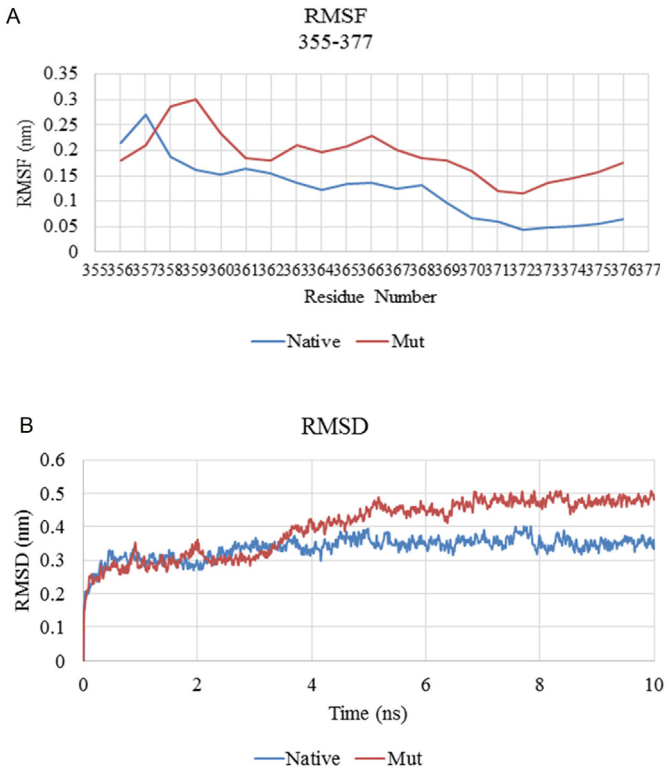

Fig. 5. Stability analysis of secondary structure. (A) The time evolutions of root-mean square deviations (RMSD) of the C-α atoms as a function of time for the native GFPT2 and its mutant. (B) The root-mean square fluctuation (RMSF) of the C-α atoms as a function of residue for the 355–377 residues of the native GFPT2 and its mutant.

boundary conditions. A 1.2 nm distance cut-off was considered during calculating the short-range electrostatic interactions and the van der Waals interactions. The long range electrostatic interactions were calculated using the Particle Mesh Ewald (PME) algorithm (Darden et al., 1993). The drastically descent algorithm and a tolerance of 500 kJ mol $^{-1}$ nm $^{-1}$ were used for energy minimization of each simulation system. All systems were equilibrated for 500 ps using the NVT ensemble. NPT equilibration was applied to each system at 1 bar of pressure. To settle water molecules around the peptide, position restraints with a spring constant of 1000 kJ mol $^{-1}$ nm $^{-2}$ were placed on all heavy atoms of the protein. The bond lengths and angles of all atoms were constrained using the LINCS algorithm. A time step of 2 fs was considered, and a neighbor list was updated every 10 steps. Finally simulations was run for 10 ns for native and mutated protein (Hess et al., 1997).

2.5. Evaluation of reactive oxygen species (ROS) levels

After 2–5 days of sexual abstinence, ROS levels were assessed in both seminal fluids and washed sperm suspensions. Two categories were determined in the present study. The first group consisted of one patient from the targeted family (III-9). The second consisted of patients with a spermogram similar to those of the first group but with a different genotype for the candidate variant. ROS levels in seminal fluid and washed sperm suspensions were obtained for each sample. The ROS levels of the washed sperm suspensions were compared between the ASZ cases with homozygous wild type alleles and the ones with homozygous mutant alleles.

2.6. ROS measurement

In order to obtain seminal plasma and washed sperm suspensions, liquefied semen was centrifuged at 300*g* for 7 min. Then, the seminal plasma was separated and the remaining pellet was washed with phosphate-buffered saline (PBS) and re-suspended in 1 ml of PBS. Chemiluminescence assay used to assess the ROS levels in each aliquot with 400 µl of seminal plasma and washed sperm. The test tubes also contained 10 µl of luminol (5 mM). The negative control consisted of 400 µl of PBS and 10 µl of luminol. A positive control was prepared by topping up luminol with 50 µl of hydrogen peroxide (30%; 8.8 M). ROS production was measured by luminol-dependent chemiluminescence in luminometer (Sirius, Berthold Detection Systems GmbH, and Pforzheim, Germany), through an integrated mode for 15 min. The results were expressed as RLU/s. All the samples were measured in duplicates and the average of the readings were reported.

3. Results

3.1. Clinical investigation

After the proband (III-16) was referred for ART, a large consanguineous family with male infertility was identified. His parents were immediate cousins and four ASZ men were found in the third generation (Fig. 1). The complete andrological examination of all affected members of this family exhibited similar features to those with normal testes, vas deferens and epididymis sizes. In addition, none of them had a history of genital tract infection or any other chronic diseases such as diabetes (Table 1). The hormone levels in all affected men were within the normal range (Table 2). They showed a normal chromosomal karyotype (46; XY) and a negative SRY testing (Supplementary Table 1). Despite the normal sperm count, sperm motility analysis showed that the rapid progressive sperm (Grad A) was zero and the total sperm motility was < 15%. It was also observed that the percentage of amorphous sperm was > 70% in each affected cases. It should be noted that none of the affected individuals had leukocytospermia (Table 2).

3.2. Identification of a missense GFPT2 variant

WES screening was carried out on extracted DNA samples from the proband and two affected family members (III-2 and III-13). A minimum of 96.92% of the on-target regions with at least 20× were read and a total of 30.57 Gigabase of sequence data from three cases were generated at high quality. WES data analyses identified 240,455 variations, filtered on the basis of four delineated steps (Fig. 2). The variants with a frequency of > 0.05 in dbSNP and ExAC were excluded, then, the remaining 37,482 variants were further analyzed. In all samples, 5336 variations indicating serious consequences in coding sequences were observed. Comparison between variants of three cases

Table 3
ROS measurement of seminal plasma and spermatozoa in patients with asthenozoospermia.

Samples	Genotype for c.1097G > A	Sperm count (106/ml)	PMN (106/ml)	RLU/S/106 (seminal fluid)	RLU/S/106 (spermatozoa)
Patient1(III-9)	AA	32	–	1.6	203.9
Pataint2	GG	37	–	11.7	0.2
Pataint3	GG	34	–	21.3	1.6
Pataint4	GG	32	–	26.6	5.1

and those of in-house database revealed 37 shared private variants. The analyses using an autosomal recessive mode of inheritance in the pedigree was prioritized. After these steps, a homozygous shared missense variant was identified in *GFPT2* (c.1097G > A) causing conversion of arginine to glutamine at position *366* (Fig. 3A&B). This variant was not observed in the homozygous state in our in-house databases nor in public databases. Analysis of the exome dataset using the Homozygosity Mapper algorithm showed that the *GFPT2* c.1097G > A variant is located on a region of homozygosity of chromosome 5p15.1 (Supplementary Fig. 1). Segregation analyses indicated that fertile parents are heterozygous for the variant and 11 fertile men showed their genotype status to be homozygote for the wild type allele or heterozygote for the missense variant. The results were consistent with the expected pattern for recessive inheritance (Fig. 3C and supplementary Table 2).

3.3. In silico analysis predicts the deleterious effect of GFPT2 mutation on protein function

The GFPT2 p.R366Q variant was predicted as "probably damaging" by Polyphen2, "deleterious" by Sift and "disease causing" by mutation taster (supplementary Table 3). Multiple alignments, using CLUSTALW indicated that arginine is not only conserved in several species but also is located within a highly conserved domain annotated as sugar isomerase SIS 1 in UniProt (Fig. 4A). Furthermore, the analyses conducted by HOPE software suggested that the charge of residue 366 was lost by this mutation resulting in failed interactions with other molecules. The wild-type residue forms a salt bridge with a glutamic acid at position 363. There was also a possible loss of protein interactions due to the smaller size of mutant amino acid compared to wild-type residue (Fig. 4B). Thus, the mutation introduced an amino acid with different properties in SIS 1 domain, which were predicted to damage this domain and lose its function.

3.4. Population study

Sanger sequencing in 30 Iranian infertile men with idiopathic ASZ revealed one homozygous patient with *GFPT2* (c.1097G > A) variant.

3.5. Prediction of GFPT2 missense variant on secondary structure stability

The stability of the native and mutant structure of the GFPT2 were assessed by molecular dynamics simulation on the homology modeling results. The root mean square deviation (RMSD) analysis was performed to investigate the equilibrium state of the native and mutant GFPT2. The RMSD analysis of the GFPT2 in native and mutant structures were illustrated in Fig. 5A. The enzymes reached a plateau after 5 ns and maintained it until the end of simulation time.

The root mean square fluctuation (RMSF) analysis was conducted for all the residues in each simulation complex. In order to analyze flexibility, RMSF values of wild type and mutant GFPT2 are calculated. High fluctuation can be noticed in the residues 355–377 of mutant protein (Fig. 5B).

The dictionary of secondary structure of protein (DSSP) analysis was performed to assess the impact of the mutation on the entire secondary structure of the GFPT2. As indicated in supplementary Fig. 3, the secondary structures were more preserved in native GFTP2 than those of the mutated state of the GFPT2. The helical structure of residues 354 to 367 turned into coils in simulation time in the mutated state. However, the helical structure of this region is conserved in the native state until the end of simulation time (shown in Fig. 4B).

3.6. Measurement of ROS levels

Our results indicated a difference in ROS levels between the seminal fluids and the washed sperm suspensions of the case III-9. The evaluation based on comparison of different samples of the washed sperm suspensions indicated that the ROS level in the sample with homozygous mutation was higher than those of homozygous wild type alleles. Notably, no difference was observed in ROS levels among all seminal fluid samples (Table 3).

4. Discussion

Approximately half of the ASZ cases with unknown etiology are believed to have genetic abnormalities (Bracke et al., 2018) although the genetic basis of ASZ is unclear. In this study, we identified a rare homozygous missense mutation (NM_005110.3; c.1097G > A) in the *GFPT2* gene causing a missense change (p.Arg366Gln) in a highly conserved residue located in the SIS 1 domain. The *GFPT2* mutation was considered to be the likely pathogenic variant contributing to ASZ. Co-segregation analyses indicated that five affected men in this large multiplex family carry the homozygous mutation and WES dataset of three cases revealed that the variant (c.1097G > A) resided in the large homozygous region. Furthermore, the *GFPT2* variant (c.1097G > A) in its homozygous status in men was found neither in public databases (ExAC, gnomAD and Iranome) nor in our in-house database. The absence of c.1097G > A variant in 400 ancestry-matched fertile men provided further support for causality of the *GFPT2*. Interestingly, the presence of *GFPT2* causative variant in the population-based Iranian ASZ patient group suggested that we could explain 2.8% of the unrelated ASZ cases by analyzing this gene. Finally, *in silico* analyses predicted that the p.R366Q variant would cause structural instability in mutant GFPT2 compared with the native protein. We concluded that the enzyme achieved higher total numbers of RMSD in the mutant structure than the native structure (Supplementary Fig. 2).

GFPT2 is a rate-limiting enzyme in hexosamine biosynthesis, which not only controls the flux of glucose within hexosamine pathway but also regulates the N- and O-linked glycosylation of proteins (Oki et al., 1999). GFPT2 belongs to class II of L-glutamine-dependent amidotransferase family (GATs), which employ their N-terminal cysteine to cleave the glutamine amide bonds and transfer the amide nitrogen to the substrate. The GFPT2 protein has two enzymatic domains, the N-terminal glutaminase domain, which hydrolyzes glutamine to glutamate and ammonia, and the C-terminal synthase domain with its two synthase domains (SIS 1 & SIS 2), which transfers ammonia to F6P and forms homotetramers (Durand et al., 2008). Since p.R366Q is located on the SIS 1 domain with a catalytic action as an isomerase (http://www.uniprot.org/), this variant may affect the function of the GFPT2 protein. To our knowledge, homozygous loss of function (LOF) mutations in *GFPT2* have not yet been linked to human diseases. However, short nucleotide polymorphisms (SNPs) in *GFPT2*, which increase *GFPT2* mRNA levels, have been associated with type 2 diabetes and chronic renal insufficiency (ZHANG et al., 2004). Additionally, ectopic *GFPT2* expression in lung adenocarcinoma has been shown to elevate O-linked glycosylation of oncofetal fibronectin, which in turn affects the induction of epithelial-mesenchymal transition (Alisson-silva et al., 2013).

High-throughput genomic studies have highlighted the protective function of GFPT2 against H_2O_2 toxicity (Zitzler et al., 2004). Miura et al. demonstrated that GFPT overcame the toxicity of methylmercury through enhancement of ROS production in yeasts (Miura et al., 1999). There is now little doubt that high concentrations of ROS can affect male fertility (Jedrzejowska et al., 2012). Multitude studies have demonstrated that genetic variations in the protective genes against ROS damage such as NOS (MIM # 163729), NRF2 (MIM # 600492), and SOD (MIM # 147450) are associated with male infertility (Buldreghini et al., 2010; Yu and Huang, 2015). In line with these studies, we evaluated ROS concentrations in seminal fluids and spermatozoa from our cases and detected higher ROS levels only in mutant spermatozoa. The results indicated that the p.R366Q variant probably had a significant effect on the sperm function by increasing ROS concentrations.

According to the literature, depletion of GFPT may reduce the cellular pool of uridine diphosphate *N*-acetylglucosamine (UPD-GlcNAc) and hyaluronan synthesis (Oikari et al., 2016). Hyaluronan is considered an important factor in controlling oxidative stress and modifying sperm motility and velocity (Bansal and Bilaspuri, 2010; Sariözkan et al., 2015). These reports support our hypothesis that the mutated *GFPT2* can increase the ROS levels, which in turn induces either peroxidation of unsaturated fatty acids or phosphorylation of axoneme proteins (Sariözkan et al., 2015). Both mechanisms can eventually decrease sperm motility (Agarwal et al., 2014).

5. Conclusion

Our findings demonstrated that six infertile men with ASZ carried mutations in *GFPT2*. On the basis of the current clinical investigations and genetic assessments, we postulate that elevated ROS levels and reduced sperm motility in ASZ infertile men are associated with homozygosity for a missense mutation in the *GFPT2*. Although high ROS concentrations have been associated with impaired fertility, there is controversy over selecting patients to test for ROS or antioxidant treatment. Therefore, our results may be helpful not only in enhancing our understanding of the genetic etiology of sperm motility but also in improving the diagnostic and therapeutic approaches.

Supplementary data to this article can be found online at https://doi.org/10.1016/j.gene.2019.02.060.

Acknowledgment

The present study was supported in part by a grant from the University of Sistan and Bluchestan (USB), Zahedan, Iran, a grant from the Royan Research Institute, Tehran, Iran and a grant from the Iran National Science Foundation (INSF).

Conflict of interest

The authors declare that they have no conflict of interest.

Accession number

rs193143625

References

Agarwal, A., Virk, G., Ong, C., Plessis, S.S., 2014. Effect of oxidative stress on male reproduction. World J. Mens. Heal. 32, 1–17.

Agarwal, A., Mulgund, A., Hamada, A., Chyatte, R.M., 2015. A unique view on male infertility around the globe. Reprod. Biol. Endocrinol. 13. https://doi.org/10.1186/s12958-015-0032-1.

Alisson-silva, F., Freire-de-lima, L., Donadio, J.L., Lucena, M.C., Penha, L., Dias, W.B., Todeschini, A.R., Sa, J.N., 2013. Increase of O-glycosylated oncofetal fibronectin in high glucose-induced epithelial-mesenchymal transition of cultured human epithelial cells. PLoS One 8. https://doi.org/10.1371/journal.pone.0060471.

Amiri-Yekta, A., Coutton, C., Kherraf, Z.E., Karaouzène, T., LeTanno, P., Sanati, M.H., Sabbaghian, M., Almadani, N., Gilani, M.A.S., Hosseini, S.H., Bahrami, S., Daneshipour, A., Bini, M., Arnoult, C., Colombo, R., Gourabi, H., Ray, P.F., 2016. Whole-exome sequencing of familial cases of multiple morphological abnormalities of the sperm flagella (MMAF) reveals new DNAH1 mutations. Hum. Reprod. 31, 2872–2880. https://doi.org/10.1093/humrep/dew262.

Avenarius, M.R., Hildebrand, M.S., Zhang, Y., Meyer, N.C., Smith, L.L.H., Kahrizi, K., Najmabadi, H., Smith, R.J.H., 2009. Human male infertility caused by mutations in the CATSPER1 channel protein. Am. J. Hum. Genet. 84, 505–510. https://doi.org/10.1016/j.ajhg.2009.03.004.

Bansal, A.K., Bilaspuri, G.S., 2010. Impacts of oxidative stress and antioxidants on semen functions. Vet. Med. Int. 2010. https://doi.org/10.4061/2011/686137.

Bhilawadikar, R., Zaveri, K., Mukadam, L., Naik, S., Kamble, K., Modi, D., Hinduja, I., 2013. Levels of Tektin 2 and CatSper 2 in normozoospermic and oligoasthenozoospermic men and its association with motility, fertilization rate, embryo quality and pregnancy rate. J. Assist. Reprod. Genet. 30, 1–11. https://doi.org/10.1007/s10815-013-9972-6.

Bracke, A., Peeters, K., Punjabi, U., Hoogewijs, D., Dewilde, S., 2018. A search for molecular mechanisms underlying male idiopathic infertility. Reprod. BioMed. Online 36, 327–339. https://doi.org/10.1016/j.rbmo.2017.12.005.

Buldreghini, E., Mahfouz, R.Z., Vignini, A., Mazzanti, L., Ricciardo-lamonica, G., Lenzi, A., Agarwal, A., Balercia, G., 2010. Single Nucleotide Polymorphism (SNP) of the Endothelial Nitric 31, 482–488. https://doi.org/10.2164/jandrol.109.008979.

Curi, S.M., Ariagno, J.I., Chenlo, P.H., Mendeluk, G.R., Pugliese, M.N., Sardi Segovia, L.M., Repetto, H.E.H., Blanco, A.M., 2003. Asthenozoospermia: analysis of a large population. Arch. Androl. 49, 343–349. https://doi.org/10.1080/01485010390219656.

Darden, T., York, D., Pedersen, L., 1993. Particle mesh Ewald: an N -log(N) method for Ewald sums in large systems. J. Chem. Phys. 98. https://doi.org/10.1063/1.464397.

DeLano, W., 2002. Pymol: an open-source molecular graphics tool. In: CCP4 Newsl. Protein Crystallogr. 40. pp. 82–92.

DePristo, M.a., Banks, E., Poplin, R.E., Garimella, K.V., Maguire, J.R., Hartl, C., Philippakis, A.A., del Angel, G., Rivas, M.A., Hanna, M., McKenna, A., Fennell, T.J., Kernytsky, A.M., Sivachenko, A.Y., Cibulskis, K., Gabriel, S.B., Altshuler, D., Daly, M.J., 2011. A framework for variation discovery and genotyping using next- generation DNA sequencing data. Nat. Genet. 43, 491–498. https://doi.org/10.1038/ng.806.A.

Dirami, T., Rode, B., Jollivet, M., Da Silva, N., Escalier, D., Gaitch, N., Norez, C., Tuffery, P., Wolf, J.P., Becq, F., Ray, P.F., Dulioust, E., Gacon, G., Bienvenu, T., Touré, A., 2013. Missense mutations in SLC26A8, encoding a sperm-specific activator of CFTR, are associated with human asthenozoospermia. Am. J. Hum. Genet. 92, 760–766. https://doi.org/10.1016/j.ajhg.2013.03.016.

Durand, P., Golinelli-Pimpaneau, B., Mouilleron, S., Badet, B., Badet-Denisot, M.-A., 2008. Highlights of glucosamine-6P synthase catalysis. Arch. Biochem. Biophys. 474, 302–317. https://doi.org/10.1016/j.abb.2008.01.026.

Gilissen, C., Hoischen, A., Brunner, H.G., Veltman, J.A., 2012. Disease gene identification strategies for exome sequencing. Eur. J. Hum. Genet. 20, 490–497. https://doi.org/10.1038/ejhg.2011.258.

Hess, B., Bekker, H., Berendsen, H.J.C., Fraaije, J.G.E.M., 1997. 3LINCS: a linear constraint solver for molecular simulations. J. Comput. Chem. 18, 1463–1472. https://doi.org/10.1002/(SICI)1096-987X(199709)18:12<1463::AID-JCC4>3.0.CO;2-H.

Hoover, W.G., 1985. Canonical dynamics: equilibrium phase-space distributions. Phys. Rev. A. Gen. Phys. 3, 1695–1697.

Jedrzejowska, R.W., Wolski, J.K., Hilczer, J.S., 2012. The Role of Oxidative Stress and Antioxidants in Male Fertility 60–67.

Kelley, L.A., Mezulis, S., Yates, C.M., Wass, M.N., Sternberg, M.J.E., 2015. The Phyre2 web portal for protein modelling, prediction, and analysis. Nat. Protoc. 10, 845–858.

Krausz, C., Escamilla, A.R., Chianese, C., 2015. Genetics of male infertility: from research to clinic. Reproduction 150, R159–R174. https://doi.org/10.1530/REP-15-0261.

kumar Mahat, R., Arora, M., 2016. Risk factors of cause of male infertility-a review. Biochem. Anal. Biochem. 5.

Kuo, Y.C., Lin, Y.H., Chen, H.I., Wang, Y.Y., Chiou, Y.W., Lin, H.H., Pan, H.A., Wu, C.M., Su, S.M., Hsu, C.C., Kuo, P.L., 2012. SEPT12 mutations cause male infertility with defective sperm annulus. Hum. Mutat. 33, 710–719. https://doi.org/10.1002/humu.22028.

Li, H., Durbin, R., 2009. Fast and accurate short read alignment with burrows-wheeler transform. Bioinformatics 25, 1754–1760. https://doi.org/10.1093/bioinformatics/btp324.

Luconi, M., Forti, G., Baldi, E., 2006. Pathophysiology of sperm motility. Front. Biosci. 11 (1), 1433. https://doi.org/10.2741/1894.

Mark, P., Nilsson, L., 2001. Structure and dynamics of the TIP3P, SPC, and SPC/E water models at 298 K. J. Phys. Chem. A 105, 9954–9960. https://doi.org/10.1021/jp003020w.

Matzuk, M.M., Lamb, D.J., 2008. The biology of infertility: research advances and clinical challenges. Nat. Med. 14, 1197–1213. https://doi.org/10.1038/nm.f.1895.

McKenna, A., Hanna, M., Banks, E., Sivachenko, A., Cibulskis, K., Kernytsky, A., Garimella, K., Altshuler, D., Gabriel, S., Daly, M., DePristo, A,.M., 2010. The genome analysis toolkit: a MapReduce framework for analyzing next-generation DNA sequencing data. Genome Res. 20, 1297–1303. https://doi.org/10.1101/gr.107524.110.

Miura, N., Kaneko, S., Hosoya, S., Furuchi, T., Miura, K., Kuge, S., Naganuma, A., 1999. Overexpression of L-glutamine: D-fructose-6-phosphate amidotransferase provides resistance to methylmercury in Saccharomyces cerevisiae. FEBS Lett. 61, 215–218. https://doi.org/10.1124/mol.61.4.738.

Nosé, S., Klein, M.L., 1983. Constant pressure molecular dynamics for molecular systems. Mol. Phys. An Int. J. Interface Between Chem. Phys. 50, 1055–1076.

Oikari, S., Makkonen, K., Deen, A.J., Tyni, I., Kärnä, R., Tammi, R.H., Tammi, M.I., 2016. Hexosamine biosynthesis in keratinocytes – roles of GFAT and GNPDA enzymes in the maintenance of UDP-GlcNAc content and hyaluronan synthesis. Glycobiology 26, 710–722. https://doi.org/10.1093/glycob/cww019.

Oki, T., Yamazaki, K., Kuromitsu, J., Okada, M., Tanaka, I., 1999. cDNA cloning and mapping of a novel subtype of glutamine: fructose-6-phosphate amidotransferase (GFAT2) in human and mouse. Genomics 57, 227–234.

Parrinello, M., Rahman, A., 1981. Polymorphic transitions in single crystals : a new molecular dynamics method polymorphic transitions in single crystals : a new molecular dynamics method. J. Appl. Phys. 52. https://doi.org/10.1063/1.328693.

Pereiraa, R., Oliveirab, J., Sousa, M., 2014. A molecular approach to sperm immotility in humans: a review. Med. Reprod. y Embriol. Clin. 1, 15–25. https://doi.org/10.1016/S2340-9320(15)30004-9.

Pfeifer, S., Butts, S., Dumesic, D., Fossum, G., Gracia, C., La Barbera, A., Odem, R., Pisarska, M., Rebar, R., Reindollar, R., Rosen, M., Sandlow, J., Sokol, R., Vernon, M., Widra, E., 2015. Diagnostic evaluation of the infertile male: a committee opinion. Fertil. Steril. 103, e18–e25. https://doi.org/10.1016/j.fertnstert.2014.12.103.

Sariözkan, S., Tuncer, P.B., Büyükleblebici, S., Bucak, M.N., Cantürk, F., Eken, A., 2015. Antioxidative effects of cysteamine, hyaluronan and fetuin on post-thaw semen quality, DNA integrity and oxidative stress parameters in the Brown Swiss bull.

Andrologia 47, 138–147. https://doi.org/10.1111/and.12236.
Van Der Spoel, D., Lindahl, E., Hess, B., Groenhof, G., 2005. GROMACS: fast, flexible, and free. J. Comput. Chem. 26. https://doi.org/10.1002/jcc.20291.
Venselaar, H., te Beek, T.A.H., Kuipers, R.K.P., Hekkelman, M.L., Vriend, G., 2010. Protein structure analysis of mutations causing inheritable diseases. An e-Science approach with life scientist friendly interfaces. BMC Bioinf. 11, 548. https://doi.org/10.1186/1471-2105-11-548.
Wang, K., Li, M., Hakonarson, H., 2010. ANNOVAR: functional annotation of genetic variants from high-throughput sequencing data. Nucleic Acids Res. 38, 1–7. https://doi.org/10.1093/nar/gkq603.
Xu, X., Sha, Y., Mei, L., Ji, Z., Qiu, P., Ji, H., Li, P., 2017. A familial study of twins with severe asthenozoospermia identified a homozygous. Clin. Genet. 93, 345–349. https://doi.org/10.1111/cge.13059.
Yu, B., Huang, Z., 2015. Variations in Antioxidant Genes and Male Infertility. pp. 2015.
ZHANG, H., JIA, Y., COOPER, J.J., HALE, T., ZHANG, Z., ELBEIN, S.C., 2004. Common variants in glutamine: fructose-6-phosphate amidotransferase 2 (GFPT2) gene are associated with. J. Clin. Endocrinol. Metab. 89, 748–755. https://doi.org/10.1210/jc.2003-031286.
Zitzler, J., Link, D., Schäfer, R., Liebetrau, W., Kazinski, M., Bonin-Debs, A., Behl, C., Buckel, P., Brinkmann, U., 2004. High-throughput functional genomics identifies genes that ameliorate toxicity due to oxidative stress in neuronal HT-22 cells: GFPT2 protects cells against peroxide. Mol. Cell. Proteomics 3, 834–840. https://doi.org/10.1074/mcp.M400054-MCP200.
Zuccarello, D., Ferlin, A., Cazzadore, C., Pepe, A., Garolla, A., Moretti, A., Cordeschi, G., Francavilla, S., Foresta, C., 2008. Mutations in dynein genes in patients affected by isolated non-syndromic asthenozoospermia. Hum. Reprod. 23, 1957–1962. https://doi.org/10.1093/humrep/den193.